Eksakta : Berkala Ilmiah Bidang MIPA
VOLUME 27 NO 05 2026, pp 932-944
ISSN : Print 1411-3724 — Online 2549-7464
DOI : https://doi.org/10.24036/eksakta/vol27-iss05/680

Eksakta
Berkala Ilmiah Bidang MIPA
http://www.eksakta.ppj.unp.ac.id/index.php/eksakta

Article

Utilization Of Hydroxyapatite From Catfish Bones as an Adsorbent For Copper (Cu(II)) Ions

Matlal Fajri Alif[1*], Syukri[1], Elga Joninda Putri[1]

[1]Department of Chemistry, Faculty of Science and Natural Science, Universitas Andalas, Padang, Indonesia

Article Info

Article history :
Received April 22, 2026
Revised October 18, 2026
Accepted October 22, 2026
Published October 30, 2026

Keywords :
Hydroxyapatite,
adsorption,
catfish bone,
Cu(II)

Abstract. Hydroxyapatite [$Ca_{10}(PO_4)_6(OH)_2$] is a porous calcium phosphate compound with potential as a heavy metal adsorbent. In this study, HAp was synthesized from calcined catfish bones using the sol–gel method and evaluated as an adsorbent for Cu(II) ions in aqueous solution. X-ray diffraction analysis confirmed the formation of a crystalline phase consistent with HAp, while BET analysis provided information on its surface area and porous structure. The effects of solution pH, initial Cu(II) concentration, and contact time on adsorption performance were investigated. The maximum adsorption capacity was 262.13 mg/g at pH 5, an initial Cu(II) concentration of 600 mg/L, and a contact time of 30 min. The adsorption kinetics were described by the pseudo-second-order model, while the equilibrium data fitted the Langmuir isotherm model, suggesting predominantly monolayer adsorption. These findings demonstrate the potential of catfish-bone-derived HAp as a biogenic adsorbent for Cu(II) removal from aqueous solutions.

This is an open acces article under the CC-BY license.

This is an open access article distributed under the Creative Commons 4.0 Attribution License, which permits unrestricted use, distribution, and reproduction in any medium, provided the original work is properly cited. ©2026 by author.

Corresponding Author :
Matlal Fajri Alif
Department of Chemistry, Faculty of Mathematics and Natural Science,
Universitas Andalas, Padang, Indonesia
Email : mfalif@sciunand.ac.id

1. Introduction

Industrial progress can have negative environmental impacts, such as an increase in waste production. This waste often contains harmful substances, including heavy metals [1]. Heavy metals cannot be degraded or destroyed. Some types of heavy metals that pollute the environment include arsenic (As), cadmium (Cd), chromium (Cr), cobalt (Co), copper (Cu), lead (Pb), and mercury (Hg) [2]. The threshold limit for copper content in the environment according to the World Health Organization (WHO) is a maximum of 0.05–1.5 mg/L. According to Government Regulation No. 22 of 2021

concerning the implementation of environmental protection and management, the limit is 0.02–0.2 mg/L. Exposure to high doses can cause health problems [3]. Therefore, measures are needed to reduce heavy metal pollution.

Several methods can be used, such as chemical precipitation, ion exchange, adsorption, and solvent extraction [4]. Adsorption is considered one of the most effective methods because it is easy to perform, highly efficient, and low-cost [2]. Adsorption requires an adsorbent. This study utilizes catfish bone waste, which was synthesized into hydroxyapatite ($Ca_{10}(PO_4)_6(OH)_2$) to be used as an adsorbent for heavy metals like copper. Based on previous research, the efficiency of heavy metal absorption with hydroxyapatite was found to be 89.5%.

Hydroxyapatite has surface active sites, such as P-OH functional group, making it ideal for binding metal cations. It has a Ca/P molar ratio of 1.67 [5] and a stable crystal structure [6]. Natural materials have been used as calcium sources for hydroxyapatite synthesis, such as chicken eggshells [7], cow bones [8], gurame fish bones [1] fish scales [9], catfish bones [10], and shell [11].

Based on data from the Ministry of Marine Affairs and Fisheries of the Republic of Indonesia, catfish production in 2021 reached 1,041,422 tons. The proportion of fish bones to fish bodies is 12.4%. Thus, catfish solid waste in Indonesia in 2022 is estimated to be 129,136 tons [10], highlighting the significant potential of using catfish bone waste as a precursor source of $CaCO_3$ for producing hydroxyapatite as a Cu metal adsorbent.

Several methods can be used for hydroxyapatite (HAp) synthesis, such as precipitation and sol-gel [12], microwave irradiation [13], and heat treatment [14]. This sol-gel method can increase the crystallinity of hydroxyapatite, produce a homogeneous layer, takes place at low temperatures, and is relatively easy to implement at a lower cost [15]. Based on a literature search, no studies were found on the synthesis of hydroxyapatite from catfish bones using the sol-gel method for Cu metal absorption. Therefore, this study employs the sol-gel method to synthesize HAp from catfish bones as a source of $CaCO_3$, with the addition of $(NH_4)_2HPO_4$ salt, which will be applied for Cu(II) metal absorption.

2. Experimental Section

2.1 Materials

The materials used in this study included catfish bones, diammonium phosphate ($(NH_4)_2HPO_4$), ammonium hydroxide (NH_4OH), nitric acid (HNO_3), potassium nitrate (KNO_3), sodium hydroxide (NaOH), and copper sulfate ($CuSO_4$). All chemicals used were Merck products with pro-analysis purity, and all solutions were prepared using distilled water (H_2O). The equipment used included laboratory glassware, a mortar and pestle, an analytical balance, rotary shaker, oven, pH meter, 200 mesh sieve, hot plate with magnetic stirrer, AAS (Shimadzu AA7000G), (BET, NOVA 800, Anton Paar), XRD (D8 Advance, Bruker), and XRF (Epsilon 3XL, PANalytical).

2.2 Preparation of Calcium Precursor from Catfish Bone

The collected catfish bones were soaked in hot water and then washed with distilled water. Next, the bones were dried in an oven at 120 °C and ground until smooth. The resulting bone powder was sieved using a 200-mesh sieve and then calcined at 900 °C for 5 hours. The CaO powder obtained from the catfish bones was used as the calcium precursor for the hydroxyapatite synthesis.

2.3 Synthesis of Hydroxyapatite (HAp)

Hydroxyapatite (HAp) was synthesized from CaO obtained from catfish bones using the sol-gel method. A Ca/P molar ratio of 1.67 was used. Briefly, 4 g of CaO was added to 75 mL of 2 M HNO_3 and stirred at 65 °C for 15 min at 250 rpm to form a $Ca(NO_3)_2$ solution. NH_4OH was then added until the pH reached 11. Subsequently, 5.1348 g of $(NH_4)_2HPO_4$ dissolved in 250 mL of distilled water was added dropwise at 60 °C under continuous stirring. The mixture was stirred at 60 °C for 5 h. The

resulting product was filtered, dried at 110 °C for 5 h, and calcined at 600 °C for 3 h to obtain HAp powder.

2.4 Material Characterization

X-ray fluorescence (XRF) was used to determine the elemental composition of the catfish bones, particularly their calcium content, to assess their suitability as a calcium precursor for HAp synthesis. The crystalline phase of the synthesized HAp was characterized by X-ray diffraction (XRD) using Cu-Kα radiation over a 2θ range of 10° - 90°. The resulting diffractogram was compared with the reference pattern of hydroxyapatite (JCPDS 00-040-0502) to identify the crystalline phase. The specific surface area, pore volume, and pore-size distribution were determined by N_2 adsorption-desorption analysis using the Brunauer-Emmett-Teller (BET) method.

2.5 pH_{pzc} (Point Zero Charge) Study

The determination of the pH_{pzc} value was carried out by adding 0.1 g of HAp into a 100 mL Erlenmeyer flask, followed by 50 mL of a 20 mg/L $CuSO_4$ solution. The initial pH was varied in the range of 2 to 9 using 0.1 M HNO_3 and 0.1 M NaOH solutions. The mixtures were shaken for 24 hours at 100 rpm. Afterward, the final pH of each sample was recorded, and a graph was plotted between the initial pH and ΔpH (final pH – initial pH). The point where the curve intersects the ΔpH = 0 axis represents the pH_{pzc} value [16].

2.6 Adsorption Study

To determination of optimum condition for Cu(II) adsorption by HAp, the pH of the Cu(II) solution was changed (3, 4, 5, 6, 7, and 8), the initial Cu(II) concentration was changed (100 to 1000 mg/L), and the contact time was changed (15, 30, 45, 60, and 75 minutes). A 50 mL Cu(II) solution was made in a 100 mL Erlenmeyer flask. The initial pH of the solutions was altered by adding 0.1 M HNO_3 or 0.1 M NaOH. After that, each solution was combined with 0.1 g of HAp and shaken at 200 rpm. Each solution was then filtered, and AAS was used to calculate the residual lead concentration in each solution [1]. Experiments involving variations in pH, initial Cu(II) concentration, and contact time were performed in duplicate (n = 2). The results are presented as mean values, and the error bars in the corresponding graphs represent the standard deviation (SD) of the duplicate measurements. The adsorption capacity (q_e) of Cu(II) metal ions was determined Equation 1:

$$q_e = \frac{(C_0 - C_e)}{m} \times V \quad (1)$$

The removal efficiency of Cu(II) (%R) was determined using Equation 2:

$$\%R = \frac{(C_0 - C_e)}{C_0} \times 100 \quad (2)$$

Where q_e is the adsorption capacity (mg/g), $Co_0$is the initial concentration of the adsorbate (mg/L), C_e is the final concentration of the adsorbate after adsorption (mg/L), m is the mass of the adsorbent (g), V is the volume of the adsorbate solution (L), and %R is the removal efficiency (%) [17].

3. Results and Discussion

3.1 Material Characterization

X-ray fluorescence (XRF) analysis was performed on the calcined catfish bones before HAp synthesis to determine their oxide composition and assess their suitability as a calcium precursor. As presented in Table 1, CaO was the predominant reported oxide, accounting for 91.131 wt.%, whereas P_2O_5 was reported at 2.357 wt.%. The high CaO content indicates that calcined catfish bones are a potential calcium source for HAp synthesis.

Table 1. XRF results of calcined catfish bones

Component (Oxide)	Composition (%)
CaO	91.131
P_2O_5	2.357

The textural properties of the synthesized HAp were evaluated using BET analysis. As shown in Table 2, the sample exhibited a specific surface area of 32.23 m^2/g, a pore volume of 0.76 cm^3/g, and an average pore size of 5.48 nm. According to the International Union of Pure and Applied Chemistry (IUPAC), pores with widths between 2 and 50 nm are classified as mesopores. Therefore, the average pore size of the synthesized HAp falls within the mesoporous range [18].

Table 2. BET analysis results of HAp

Sample	Surface Area(m2/g)	Pore Volume (cm3/g)	Pore size (nm)
HAp	32.23	0.76	5.48

Figure 1 presents the X-ray diffraction (XRD) pattern of the HAp synthesized from calcined catfish bones. The diffraction peaks observed at approximately 25–26°, 31–33°, and 34° (2θ) are consistent with the characteristic reflections of hydroxyapatite (HAp). The experimental diffraction pattern was compared with the JCPDS standard for HAp, and the corresponding peak positions supported the identification of the HAp phase. Similar diffraction features have been reported for HAp derived from fish bones, in which the reflections around 25.9°, 31.8°, 32.2°, and 32.9° correspond to the characteristic apatite structure [19].

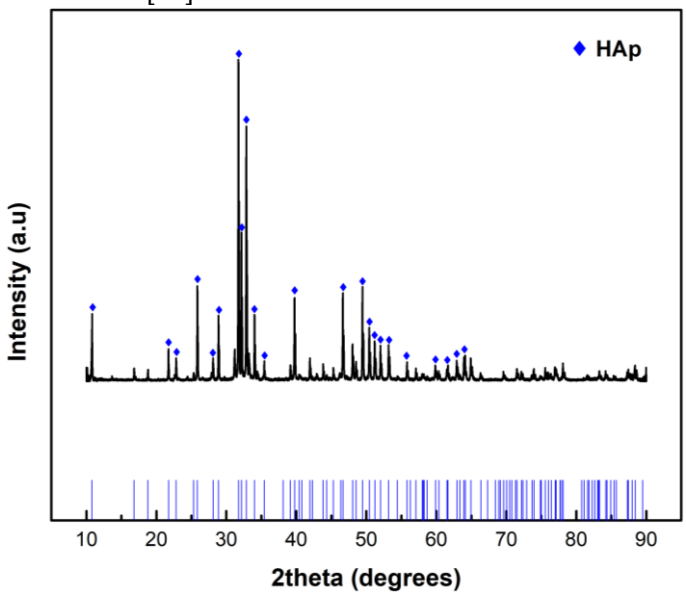


Figure 1. XRD diffraction pattern of HAp

3.2 pH_{pzc} and Its Relation to the Optimum Adsorption pH

The pH_{pzc} measurement was performed to determine the point at which the adsorbent's surface charge is neutral. The pH_{pzc} value is obtained from the plot of initial pH versus ΔpH, specifically at the intersection point where ΔpH = 0 [20]. The results (Figure 2) show that the pHpzc of hydroxyapatite is at pH 7, indicating its surface is neutrally charged under these conditions. Cation adsorption increases when pH > pH_{pzc} because the adsorbent surface is negatively charged, whereas at pH < pH_{pzc}, the surface is positively charged and tends to adsorb anions [21].

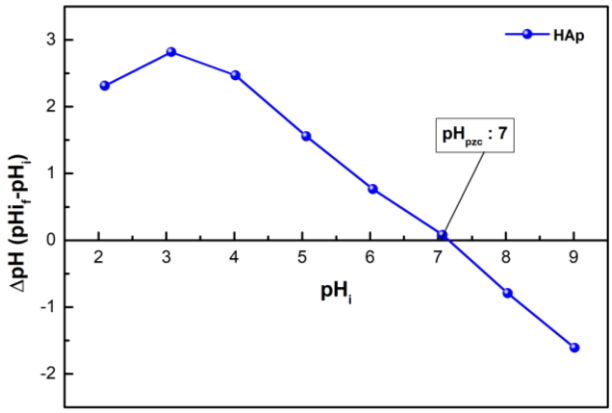


Figure 2. pH_{pzc} of Hydroxyapatite from catfish bones

Interestingly, the optimum Cu(II) adsorption in this study was obtained at pH 5, which is below the pH_{pzc} (pH 7) where the HAp surface is expected to be net positively charged. This apparent discrepancy indicates that simple electrostatic attraction is not the dominant uptake mechanism for Cu(II) on HAp. Instead, Cu(II) removal below pH_{pzc} is consistent with a specific chemisorption pathway: ion exchange between surface Ca^{2+} and Cu^{2+}, and surface complexation of Cu^{2+} with structural $PO4^{3-}$ and OH^{-} groups, which can proceed even on a nominally positively charged surface because it does not rely solely on long-range electrostatic attraction. This is consistent with the low pH range (3–5) in which adsorption capacity was still found to increase (Section 3.3).

3.3 Effect of pH

The initial pH of the solution is a critical parameter, as it determines the surface charge of the adsorbent and the degree of ionization of the metal ions to be adsorbed [22]. As shown in Figure 3, Cu(II) adsorption by catfish-bone hydroxyapatite (HAp) increased as the initial pH increased from 3 to 5, reaching an optimum adsorption capacity of 9.08 mg/g and an adsorption efficiency of 90.84% at pH 5. Under strongly acidic conditions, excess H^{+} ions may compete with Cu^{2+} for available adsorption sites, including surface hydroxyl and phosphate groups. Increasing the pH reduces the H^{+} concentration and may therefore alleviate this competition, promoting Cu(II) uptake.

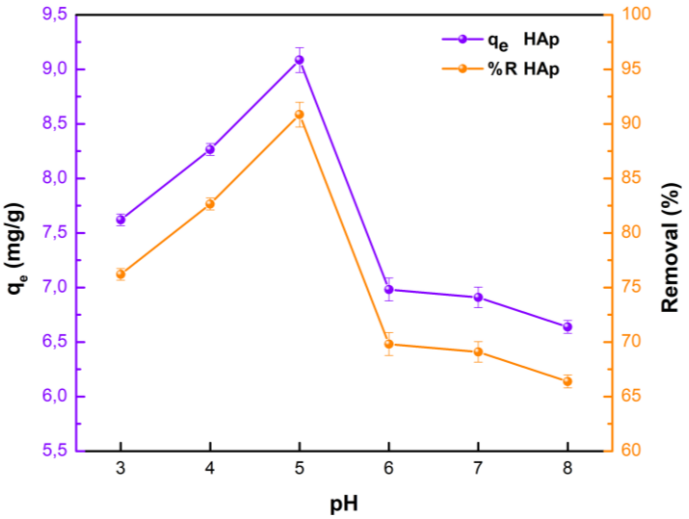


Figure 3. Impact of pH on the Adsorption Ability of HAp

Note : (C_0 = 20 mg/L; V = 50 mL; adsorbent mass = 0.1 g; t = 60 min; stirring speed = 200 rpm; n = 2)

Above pH 5, the adsorption performance decreased slightly. To further examine the possible contribution of aqueous copper speciation, a Cu(II) speciation diagram was generated using Visual MINTEQ (Figure 4). The simulation indicates that Cu^{2+} is the predominant dissolved species under acidic conditions, accounting for approximately 94.95% of total dissolved copper at pH 5. Its proportion decreases markedly as the pH increases, reaching approximately 36.80% at pH 7 and 2.67% at pH 8. In contrast, the proportions of hydrolyzed and polynuclear copper species increase with increasing pH. $CuOH^{+}$ reaches a maximum proportion of approximately 10.53% at pH 7, whereas $Cu(OH)_{2(aq)}$ increases gradually but remains a minor dissolved species, accounting for approximately 1.38% at pH 8. The polynuclear species $Cu_2(OH)_2^{2+}$ and $Cu_3(OH)_4^{2+}$ also become increasingly important at higher pH values. In particular, $Cu_3(OH)_4^{2+}$ becomes the predominant species in the simulated dissolved copper distribution at pH 8, accounting for approximately 70.85%.

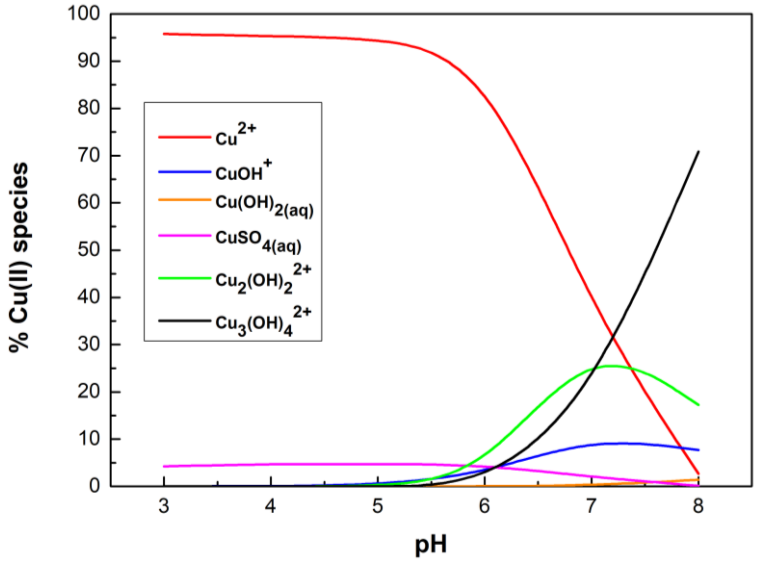


Figure 4. Visual MINTEQ-predicted aqueous speciation of Cu(II) as a function of pH (3–8). Species distributions are expressed as percentages of total dissolved copper, with the contributions of polynuclear complexes calculated by accounting for the number of Cu atoms in each species.

These results demonstrate that increasing pH changes the distribution of dissolved Cu(II) species from predominantly free Cu^{2+} toward hydrolyzed and polynuclear forms. This change may influence the interactions between dissolved copper and the HAp surface and may partly contribute to the observed pH-dependent adsorption behavior. Nevertheless, the speciation diagram alone cannot establish that the decrease in adsorption above pH 5 is caused by the formation of these species, because their relative adsorption affinities were not directly determined. Furthermore, $Cu(OH)_{2(aq)}$, shown in the diagram, represents a dissolved species and should not be interpreted as evidence of solid $Cu(OH)_2$ precipitation.

The possibility of precipitation at higher pH requires separate evaluation of the relevant solid-phase saturation conditions. Overall, pH 5 was identified as the optimum condition for Cu(II) adsorption by HAp in this study. At this pH, free Cu^{2+} remains the dominant dissolved species, while the concentration of competing H_+ ions is lower than under more acidic conditions. The observed optimum therefore reflects the combined influence of solution acidity, adsorbent–solute interactions, and aqueous copper speciation rather than a single mechanism.

3.4 Effect of Concentration and Isotherm Study

This experiment aims to determine the relationship between the number of active sites on the adsorbent surface and the increase in solution concentration. The results are shown in Figure 5.

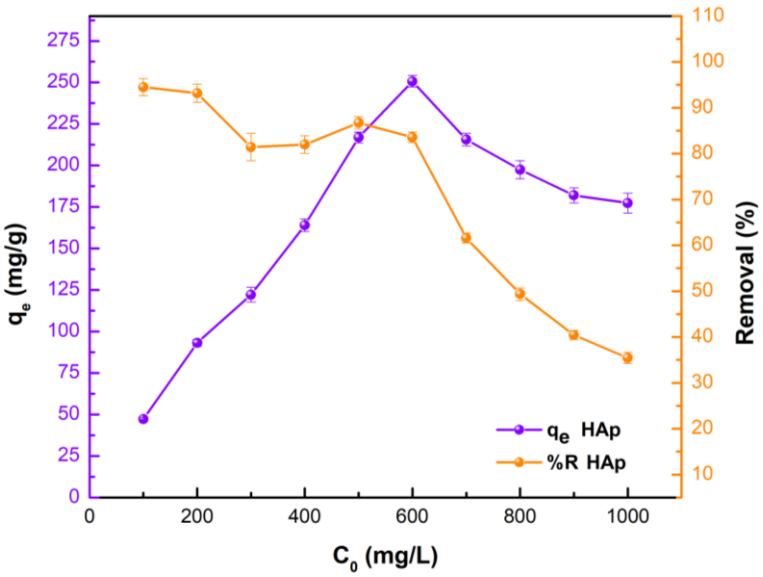


Figure 5. Impact of Cu(II) Concentration on the Adsorption Ability of HAp
Note : (pH = 5; V = 50 mL; adsorbent mass = 0.1 g; t = 60 min; stirring speed = 200 rpm; n = 2)

Figure 5 illustrates the effect of the initial Cu(II) concentration on the adsorption performance of catfish-bone hydroxyapatite (HAp). The adsorption capacity increased with increasing initial Cu(II) concentration from 100 to 600 mg/L, reaching a maximum value of 250.68 mg/g at 600 mg/L, with a removal efficiency of 83.56%. This increase can be attributed to the enhanced concentration gradient between the bulk solution and the adsorbent surface, which provides a stronger driving force for Cu(II) mass transfer toward the adsorption sites. The higher availability of Cu(II) ions in solution consequently promotes greater uptake by HAp [23].

At initial concentrations above 600 mg/L, the adsorption capacity decreased, accompanied by a decline in removal efficiency. This behavior indicates that increasing the initial Cu(II) concentration beyond 600 mg/L did not result in a further increase in the amount of Cu(II) adsorbed per unit mass of HAp under the experimental conditions. Although a limited number of available adsorption sites can restrict further uptake at high concentrations, site saturation alone would generally be expected to produce a plateau rather than a decrease in adsorption capacity. Therefore, the observed decline may reflect additional concentration-dependent effects within the adsorption system. However, the specific mechanism responsible for this decrease cannot be established from the concentration-dependent adsorption results alone and requires further investigation [24].

Adsorption isotherm models are used to describe the interaction between adsorbate and adsorbent at equilibrium. The Langmuir and Freundlich models were used to determine the adsorption parameters [25], with the better-fitting model selected based on the coefficient of determination (R^2) closest to one [26]. The adsorption process creates a monolayer at uniform active sites, as explained by the Langmuir model. Since the active sites on the adsorbent surface are already completely covered when Cu(II) ions occupy them, further adsorption is not possible. In contrast, the Freundlich model postulates that the adsorption process occurs on a multilayer surface, contingent upon the interaction between the adsorbent surface and the adsorbate [27]. The Langmuir and Freundlich models were used to evaluate the Cu(II) adsorption equilibrium data by HAp, as shown

in Figure 6. The parameters obtained from Langmuir and Freaundlich isotherm models are summarized in Table 3.

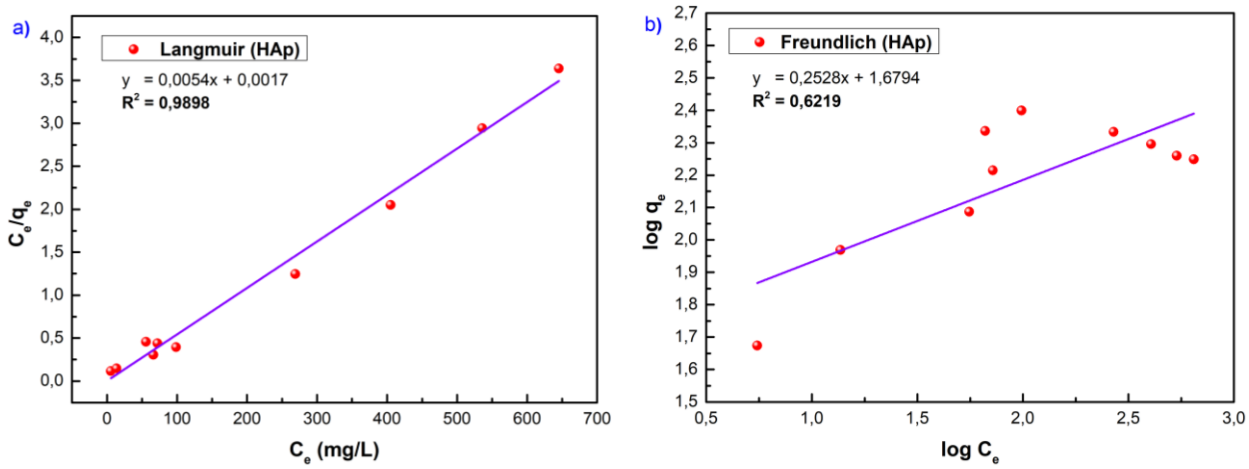


Figure 6. Fitting plots of (a) Langmuir and (b) Freundlich isotherm models

Based on the R^2 values reported, the Langmuir model yielded an R^2 value of 0.9898, which was higher than that obtained for the Freundlich model (0.6219), indicating that the Langmuir model provided a better fit to the data using the regression approach applied in this study. The Langmuir model assumes monolayer adsorption on a surface with a finite number of adsorption sites that are equivalent in terms of adsorption energy [28]. The estimated maximum adsorption capacity was 185.1852 mg/g, while the Langmuir constant K_L was 3.1765 L/mg. The dimensionless separation factor R_L ranged from approximately 0.0003 to 0.0031, indicating favorable adsorption according to the Langmuir model, provided that the fitted parameters and calculation inputs are correct. In comparison, the Freundlich model yielded a lower R^2 of 0.6219 and a 1/n value of 0.2528. The positive 1/n value is consistent with favorable adsorption according to the conventional Freundlich interpretation, although the lower R^2 indicates that this model described the experimental data less well than the Langmuir model.

Table 3. Langmuir and Freundlich Parameters for Cu(II) Sorption by HAp

Isotherm model	Equation	Parameters	Result
Langmuir	$\frac{C_e}{q_e} = \frac{1}{K_L q_m} + \frac{C_e}{q_m}$	q_m (mg g^{-1})	185.1852
		K_L (L mg^{-1})	3.1765
		R_L	0,0003-0,0031
		R^2	0.9898
Freundlich	$\log q_e = \log K_F + \log C_e$	K_F	5.3623
		1/n	0.2528
		R^2	0.6219

3.5 Effect of Contact Time and Kinetics Study

The determination of contact time aims to find out the minimum time required for HAp to adsorb Cu(II) metal ions. The analysis results are shown in Figure 7.

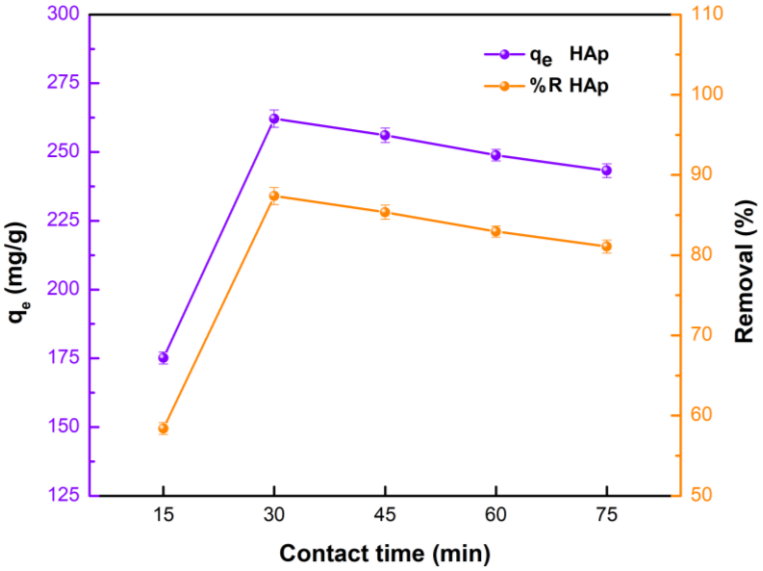


Figure 7. Effect of Contact Time on the Adsorption of Cu(II) by HAp

Note : (pH = 5; C_0 = 600 mg/L; V = 50 mL; adsorbent mass = 0.1 g; stirring speed = 200 rpm; n = 2)

As shown in Figure 7, the adsorption capacity and removal efficiency increased significantly as the contact time increased from 15 to 30 min. The optimum adsorption performance was achieved at 30 min, with an adsorption capacity of 262.13 mg/g and a Cu(II) removal efficiency of 87.38%. Beyond this point, both parameters gradually decreased as the contact time increased from 45 to 75 min. This trend suggests that the adsorption process reached its maximum performance at 30 min under the experimental conditions. The subsequent decrease may be associated with changes in the adsorption–desorption equilibrium or the redistribution of adsorbed Cu(II) ions. Further kinetic analysis is required to determine the adsorption mechanism and the model that best describes the experimental data.

Adsorption kinetics models analyze the relationship between contact time and the amount of adsorbate adsorbed. The two commonly used models are pseudo-first-order and pseudo-second-order [29]. As shown in Figure 8 and Table 4, the pseudo-first-order model exhibited a coefficient of determination R^2 of 0.002, with a calculated equilibrium adsorption capacity of 12.1630 mg/g. In contrast, the pseudo-second-order model yielded a substantially higher R^2 value of 0.9828 and a calculated equilibrium adsorption capacity of 263.1579 mg/g, which is close to the experimental adsorption capacity of 262.13 mg/g. These results indicate that the pseudo-second-order model provides a better fit to the experimental data than the pseudo-first-order model.

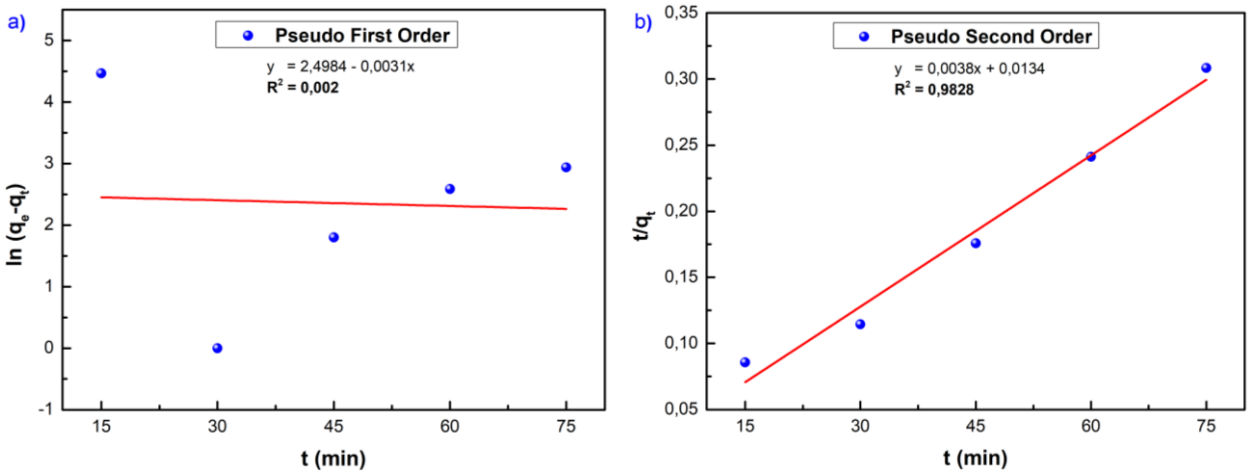


Figure 8. Fitting plots of (a) pseudo-first-order and (b) pseudo-second-order kinetic models

The agreement between the calculated and experimental adsorption capacities further supports the suitability of the pseudo-second-order model for describing the adsorption kinetics under the investigated conditions, suggesting that the adsorption mechanism is dominated by chemisorption most likely ion exchange between surface active groups (OH and $PO4^{3-}$) and Cu(II) ions, consistent with the mechanism discussed in Section 3.2. However, the kinetic model alone does not conclusively establish the adsorption mechanism; additional characterization and mechanistic evidence are required to confirm the specific interactions between Cu(II) ions and the functional groups of HAp.

Table 4. Kinetic model parameters for the adsorption of Cu(II) by HAp

Kinetic model	Equation	Parameters	Result
Pseudo First Order	$\ln(q_e-q_t)= \ln q_e - \frac{k_1 t}{2.303}$	K_1 (min^{-1})	0.0071
		q_e calc (mg g^{-1})	12.1630
		R^2	0.002
Pseudo Second Order	$\frac{t}{q_t} = \frac{1}{k_2 q_e^2} + \frac{t}{q_e}$	K_2 (g $mg^{-1}min^{-1}$)	0.0011
		q_e calc (mg g^{-1})	263.1579
		R^2	0.9828
q_e experiment		q_{exp} (mg/g)	262.13

3.6 Application in Teluk Bayur Water

The adsorption performance of hydroxyapatite (HAp) was evaluated using Teluk Bayur water under the optimum conditions of pH 5 and a contact time of 30 min. The experiments were performed in duplicate, and the initial and final Cu(II) concentrations, adsorption capacity, and removal efficiency were determined. The results are presented in Table 5.

Table 5. Results of applying optimum conditions for Cu(II) metal adsorption by HAp to water samples

	pH	Contact time	C_o (mg/L)	C_e (mg/L)	%R	SD
Cu(II)	5	30 min	1.6844	0.1714	89.82%	±0.0070

As shown in Table 4, HAp achieved a Cu(II) removal efficiency of 89.82% and an adsorption capacity of 0.7565 mg/g. According to Government Regulation of the Republic of Indonesia No. 22 of 2021, the Cu concentration limit depends on the designated water quality class. Therefore, the final Cu(II) concentration should be compared with the applicable standard to evaluate treatment performance. In addition, competing ions such as Ca^{2+}, Mg^{2+}, and Fe species may affect Cu(II) adsorption through competition for active sites. However, their effects could not be confirmed because their concentrations were not measured.

3.7 Adsorption-Desorption Study

Adsorption–desorption cycle was performed to evaluate the biosorbent's regeneration ability and reusability for large-scale applications [30]. Reusing the biosorbent makes the adsorption process more economical by reducing costs. The reused biosorbent was regenerated by contacting it with a desorbing agent. The desorbing agent should be effective, environmentally friendly, and low-cost. Putra [16] previously reported using 0.01 M HNO_3 as an effective desorbing agent.

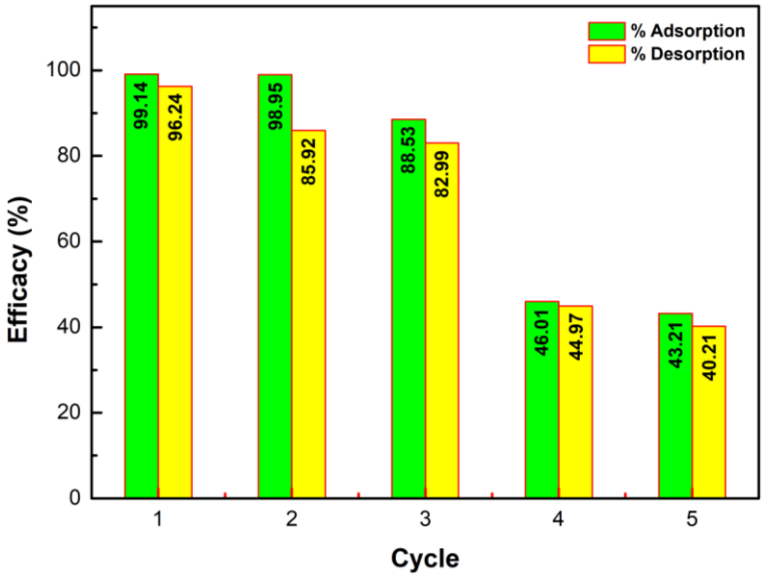


Figure 9. Reusability of HAp

Figure 9 shows the adsorption–desorption performance of HAp over five consecutive cycles. The adsorption efficiency decreased from 99.14% in the first cycle to 88.63% in the third cycle, followed by a substantial decline to 46.01% and 43.21% in the fourth and fifth cycles, respectively. Similarly, the desorption efficiency decreased from 96.24% to 40.21% over the five cycles. These results indicate that HAp maintained high adsorption efficiency during the initial cycles, but its performance declined considerably upon repeated regeneration.

4. Conclusion

Catfish bones were successfully used as a calcium precursor for the sol–gel synthesis of hydroxyapatite (HAp). Under the investigated conditions, the highest experimental Cu(II) adsorption capacity was 262.13 mg/g at pH 5, an initial Cu(II) concentration of 600 mg/L, and a contact time of 30 min. The pseudo-second-order kinetic model provided a better fit to the experimental kinetic data than the pseudo-first-order model, while the Langmuir model fitted the equilibrium data better than the Freundlich model based on the reported coefficients of determination.

The adsorption efficiency decreased substantially during five consecutive adsorption–desorption cycles, from 99.14% in the first cycle to 43.21% in the fifth cycle. Because post-cycle XRD and SEM analyses were not performed, the cause of this decline and the structural stability of the regenerated HAp remain unconfirmed. Further validation of the isotherm parameters and the real-water application results is required before drawing firm conclusions about the adsorbent's practical performance.

References

[1] R. F. Diba, V. Amalia, E. P. Hadisantoso, and Y. Rohmatulloh. (2019). Adsorpsi Ion Logam Tembaga(II) dalam Air Dengan Serbuk Tulang Ikan Gurame (Osphronemus gourami Lac). *al-Kimiya*, vol. 4, no. 2, pp. 105–112.

[2] Z. Raji, A. Karim, A. Karam, and S. Khalloufi. (2023). Adsorption of Heavy Metals: Mechanisms, Kinetics, and Applications of Various Adsorbents in Wastewater Remediation—A Review. *Waste*, vol. 1, no. 3, pp. 775–805.

[3] S. M. Javad Sajjadi Shourije *et al.* (2022). Using fish scales as a new biosorbent for adsorption of nickel and copper ions from wastewater and investigating the effects of electric and magnetic fields on the adsorption process. *Chemosphere*, vol. 317.

[4] N. K. Gupta, A. Gupta, P. Ramteke, H. Sahoo, and A. Sengupta. (2019). Biosorption-a green method for the preconcentration of rare earth elements (REEs) from waste solutions: A review. *J. Mol. Liq.*, vol. 274.

[5] M. F. Alif, W. Aprillia, and S. Arief. (2018). Peat Water Purification by Hydroxyapatite (HAp) Synthesized from Waste Pensi (Corbicula moltkiana) Shells. *IOP Conf. Ser. Mater. Sci. Eng.*, vol. 299, no. 1.

[6] T. Windarti, A. S. Setiadi, F. Fibriani, I. M. A. Azis, and S. A. Putri. (2024). Sintesis dan Karakterisasi Hidroksiapatit dengan Metode Sol-Gel Sebagai Bahan Dasar Adsorben. *Greensph. J. Environ. Chem.*, vol. 3, no. 2.

[7] M. Akram, R. Ahmed, I. Shakir, W. A. W. Ibrahim, and R. Hussain. (2014). Extracting hydroxyapatite and its precursors from natural resources. *J. Mater. Sci.*, vol. 49, no. 4.

[8] V. Amalia, E. P. Hadisantoso, D. Hidayat, R. F. Diba, and M. F. Dermawan. (2018). Isolasi dan Karakterisasi Hidroksiapatit dari Limbah Tulang Hewan. vol. 4.

[9] M. A. Selimin, A. F. A. Latif, C. W. Lee, M. S. Muhamad, H. Basri, and T. C. Lee. (2022). Adsorption efficiency of hydroxyapatite synthesised from black tilapia fish scales for chromium (VI) removal. *Mater. Today Proc.*, vol. 57.

[10] M. Primawestri, Sumardianto, and R. A. Kurniasih. (2023). Karakteristik Stik Ikan Lele (Clarias gariepinus) Dengan Perbandingan Rasio Daging dan Tulang. *J. Ilmu dan Teknol. Perikan.*, vol. 5, no. 1, pp. 1–23, 2023.

[11] J. Joe Pushba Shini *et al.* (2024). Synthesis of hydroxyapatite (HAp) from eggshells via thermal decomposition method for the application of dye adsorption. *J. Indian Chem. Soc.*, vol. 101, no. 10.

[12] T. Charlena, Maddu, A., & Hidayat. (2022). Synthesis and Characterization of Hydroxyapatite from Green Mussel Shell with Sol-Gel Method. *J. Kim. Val.*, vol. 8(2).

[13] M. A. M. Castro, T. O. Portela, G. S. Correa, M. M. Oliveira, J. H. G. Rangel, S. F. Rodrigue, J. M. R. Mercury. (2022). Synthesis of hydroxyapatite by hydrothermal and microwave irradiation methods from biogenic calcium source varying pH and synthesis time. *Boletín la Soc. Española Cerámica y Vidr.*, vol. 61, no. 1, pp. 35–41.

[14] B. R. Sunil and M. Jagannatham. (2016). Producing hydroxyapatite from fish bones by heat treatment. *Mater. Lett.*, vol. 185, no. August, pp. 411–414.

[15] Sumarto, Desmelati, N. I. Sari, R. M. Angraini, and L. Arieska. (2021). Characteristic of Nano-Calcium Bone from a Different Species of Catfish (Pangasius hypophthalmus, Clarias

batrachus, Hemibagrus nemurus and Paraplotosus albilabris). *IOP Conf. Ser. Earth Environ. Sci.*, vol. 695, no. 1, pp. 1–9.

[16] A. Putra, S. Fauzia, D. Deswati, S. Arief, and R. Zein. (2024). The potential of duck egg white as a modifier for activated rice straw to enhance Cr(VI) ions adsorption in an aqueous solution. *South African J. Chem. Eng.*, vol. 48, pp. 204–213.

[17] L. Hevira, Zilfa, Rahmayeni, J. O. Ighalo, H. Aziz, and R. Zein. (2021). Terminalia catappa shell as low-cost biosorbent for the removal of methylene blue from aqueous solutions. *J. Ind. Eng. Chem.*, vol. 97, pp. 188–199.

[18] M. Thommes *et al.* (2015). Physisorption of gases, with special reference to the evaluation of surface area and pore size distribution (IUPAC Technical Report). vol. 87, pp. 1051–1069.

[19] P. Shi, M. Liu, F. Fan, C. Yu, W. Lu, and M. Du. (2018). Materials Science & Engineering C Characterization of natural hydroxyapatite originated from fish bone and its biocompatibility with osteoblasts. *Mater. Sci. Eng. C*, vol. 90, no. April, pp. 706–712.

[20] E. A. Al-Maliky, H. A. Gzar, and M. G. Al-Azawy. (2021). Determination of Point of Zero Charge (PZC) of Concrete Particles Adsorbents. *IOP Conf. Ser. Mater. Sci. Eng.*, vol. 1184, no. 1.

[21] D. Pal and S. K. Maiti. (2019). An approach to counter sediment toxicity by immobilization of heavy metals using waste fish scale derived biosorbent. *Ecotoxicol. Environ. Saf.*, vol. 187.

[22] A. Vahdat, B. Ghasemi, and M. Yousefpour. (2019). Syntehsis oh Hydroxyapatite and Hydroxyapatite/FeO3 nanocomposite for Removal of Heavy Metals. *Enviromental Nanotechnology, Monit. Manag.*, vol. 4, no. 2, pp. 86–97.

[23] A. Alamin. (2016). Removal of Pb (II) from Aqueous Solutions Using Mixtures of Bamboo Biochar and Calcium Sulphate, and Hydroxyapatite and Calcium Sulphate. *Environ. Kaewsichan, Lupong*.

[24] E. Nasution, A. N., Amrina, Y., Zein, R., Aziz, H., & Munaf. (2015). Biosorption characteristics of Cd (II) ions using herbal plant of mahkota dewa (Phaleria macrocarpa). *J. Chem. Pharm. Res.*, vol. 7(7), pp. 189–196.

[25] C. A. Riyanto and E. Prabalaras. (2019). The adsorption kinetics and isoterm of activated carbon from Water Hyacinth Leaves (Eichhornia crassipes) on Co(II). *J. Phys. Conf. Ser.*, vol. 1307, no. 1.

[26] R. Zein, P. Ramadhani, H. Aziz, and R. Suhaili. (2019). Pensi shell (Corbicula moltkiana)as a biosorbent for metanil yellow dyes removal: pH and equilibrium model evaluation. *J. Litbang Ind.*, pp. 15–22.

[27] S. Abbas, T. Javeed, S. Zafar, M. B. Taj, A. R. Ashraf, and M. I. Din. (2021). Adsorption of crystal violet dye by using a low-cost adsorbent – peanut husk. *Desalin. Water Treat.*, vol. 233, pp. 387–398.

[28] D. Shi *et al.* (2021). Optimization of hydrothermal synthesis of hydroxyapatite from chicken eggshell waste for effective adsorption of aqueous Pb(II). *Environ. Sci. Pollut. Res. Int.*, vol. 28, no. 41, pp. 58189–58205.

[29] A. Tenea *et al.* (2024). Heliyon Exploring adsorption dynamics of heavy metals onto varied commercial microplastic substrates : Isothermal models and kinetics analysis. *Heliyon*, vol. 10, no. 15.

[30] N. Khadhri, M. El Khames Saad, M. Ben Mosbah, and Y. Moussaoui. (2019). Batch and continuous column adsorption of indigo carmine onto activated carbon derived from date palm petiole. *J. Environ. Chem. Eng.*, vol. 7, no. 1.